THE JOURNAL OF PHYSICAL CHEMISTRY C

C: Surfaces, Interfaces, Porous Materials, and Catalysis

Acetonitrile Adsorption on Pt Single Crystal Electrodes and Its Effect on the Oxygen Reduction Reaction in Acidic and Alkaline Aqueous Solutions

Valentin Briega-Martos, Marta Costa-Figueiredo, Jose Manuel Orts, Antonio Rodes, Marc T.M. Koper, Enrique Herrero, and Juan M. Feliu

J. Phys. Chem. C, **Just Accepted Manuscript** • Publication Date (Web): 01 Jan 2019

Acetonitrile Adsorption on Pt Single Crystal Electrodes and its Effect on the Oxygen Reduction Reaction in Acidic and Alkaline Aqueous Solutions

Valentín Briega-Martos[1], Marta Costa-Figueiredo[2,3], José M. Orts[1], Antonio Rodes[1], Marc T. M. Koper[2], Enrique Herrero[1], Juan. M. Feliu[1]*

[1]Instituto de Electroquímica, Universidad de Alicante, Apdo. 99, E-03080 Alicante, Spain

[2] Leiden Institute of Chemistry, Leiden University, PO Box 9502, 2300 RA Leiden, The Netherlands

Present address:

[3]Avantium Chemicals, Science Park 408, Matrix Building VI, 1098XH Amsterdam, The Netherlands

*Corresponding author: herrero@ua.es

Abstract

The adsorption and reactivity of acetonitrile (CH_3CN) have been studied on Pt(111) and Pt(100) electrodes in 0.1 M $HClO_4$ and 0.1 M NaOH solutions with CH_3CN concentrations ranging from 10^{-3} M to 1 M. Cyclic voltammetry results show that these processes are structure sensitive and that the hydrogen adsorption/desorption region is partially blocked on Pt(111) in acidic solutions while the inhibition is almost complete on Pt(100) in both acidic and alkaline media. However, for Pt(111) hydrogen adsorption is practically unaltered in the 0.1 M NaOH electrolyte. In-situ infrared measurements and DFT calculations suggest that rehybridized adsorbed acetonitrile reacts with adsorbed hydroxyl species at high potentials forming a hydroxylated adsorbed species. The latter is bonded to the Pt surface by electrodonation and can be reduced to an

intermediate in which the double C-N bond is tilted with respect to the metal surface. Lastly, oxygen reduction reaction (ORR) has been investigated by using the hanging meniscus rotating disk electrode (HMRDE) configuration. Limiting current densities decrease more drastically for Pt(100) than for Pt(111) as acetonitrile concentration is increased because of the higher acetonitrile coverage for the former one. The onset potential for ORR is shifted to less positive values in acidic media because of a blocking effect of acetonitrile. In alkaline media, the onset potential for Pt(111) is slightly more positive for low concentrations of acetonitrile since oxide formation, which hinders oxygen reduction for the more positive potentials, is inhibited due to the presence of acetonitrile adsorbed species at low coverages.

1. Introduction

Oxygen reduction reaction (ORR) is probably the most important cathodic process in electrocatalysis since it is involved in several applications such as fuel cells and lithium-air batteries. Unfortunately, the overpotential for this reduction reaction on Pt, the most active pure metal, is ca. -0.3 V. Therefore, the ORR still constitutes one of the main limiting factors in fuel cell technology. Generally speaking, the ORR can either produce water as the final product (Eq. 1) or yield hydrogen peroxide (H_2O_2), with only two electrons being involved in this case (Eq. 2).[1,2]

$$(1)\ O_2 + 4H^+ + 4e^- \rightleftharpoons 2H_2O \qquad E^0 = 1.229\ \text{V vs. SHE}$$

$$(2)\ O_2 + 2H^+ + 2e^- \rightleftharpoons H_2O_2 \qquad E^0 = 0.695\ \text{V vs. SHE}$$

The full mechanism is complex and the identity of all the intermediates is not totally elucidated yet. Recent works suggest that in acidic to neutral pH values the formation of a $OOH^{\bullet}$ soluble intermediate constitutes a bifurcation point in the mechanism before the step yielding H_2O_2.[3-5] As the specific mechanism depends on the

particular experimental conditions, a full understanding of the factors that govern the ORR will allow a rational design of more efficient new electrocatalysts for this reaction.

The study of the effect of organic molecules on the ORR can be useful for the improvement of the above-mentioned technologies. On the one hand, in Li-O_2 batteries research field it is mandatory to study the O_2 reduction reaction in aprotic organic solvents. On the other hand, organic compounds present in ambient air can contaminate the Pt/C catalyst used in proton-exchange membrane fuel cells (PEMFCs) due to the high electrocatalytic activity of Pt [6]. Acetonitrile (CH_3CN) is one of the simplest organic molecules that can take part in those processes and the study of its surface electrochemistry and electrocatalytic effects toward the ORR can provide some interesting fundamental knowledge on the effect of the interfacial properties on the electrocatalysis.

Acetonitrile electrochemistry on Pt surfaces was first studied by Angerstein-Kozlowska et al.[7] who observed in cyclic voltammetry experiments that acetonitrile is chemisorbed from aqueous solutions over a potential range ranging from 0.05 to ca. 0.75 V vs. RHE (reversible hydrogen electrode) showing almost reversible reduction/oxidation processes. This was one of the first examples of a chemically modified electrode. In order to obtain more information about the adsorbed species and the processes that occur on the Pt surface, Morin et al.[8,9] investigated the electrochemical behavior of acetonitrile on well-oriented surfaces. They found that acetonitrile adsorption processes and surface reactivity resulted to be structure sensitive as pointed out by cyclic voltammetry experiments.[8] These authors concluded that acetonitrile is adsorbed at potentials above 0.60 V vs. RHE and undergoes a first one-electron reduction step between 0.60 and 0.36 V vs. RHE followed by further reduction at lower potentials. They proposed that during the first reduction process, adsorbed

acetonitrile would re-orientate with a change of the triple CN bond into a double bond. This reduced adsorbed intermediate could be reversibly re-oxidized above 0.35 V vs. RHE. The interface between Pt electrodes and an acetonitrile-containing electrolyte solution was studied by in-situ external reflection infrared spectroscopy for the first time by Marinković et al.[10] They proposed a reorientation of the acetonitrile bonded to the metal surface by the nitrogen lone electron pair to yield a re-hybridized species with the C-N bond parallel to the surface.[10] Morin *et al.* also performed in-situ infrared measurements and proposed the formation, from the re-hybridized acetonitrile, of a reduced intermediate in which the double C-N bond would be tilted with respect to the surface plane, making its stretching mode to be infrared active.[9] However, that tentative explanation relied on band assignments based on the comparison of the observed band frequencies with previous data from iron complexes and UHV experiments.[11,12] Therefore, the exact nature of the formed intermediates is not totally clear yet. The in-situ infrared study of acetonitrile adsorption on polycrystalline and stepped Pt surfaces in aqueous sulfuric acid solutions yielded bands similar to those observed in the works mentioned above.[13] The electrochemical behavior of Pt surfaces in acetonitrile electrolytes with different amounts of water was studied by Suárez-Herrera et al., who observed, by cyclic voltammetry and infrared measurements, that adsorbed acetonitrile can be reduced and then re-oxidized reversibly with little desorption.[14] It was also pointed out that the interactions of interfacial water with the reacting species and with the electrode surface have an influence on the observed electrocatalytic processes, even at very high acetonitrile concentrations.[15,16]

For the sound interpretation of the infrared spectra of adsorbed species, theoretical studies are normally carried out to obtain calculated band frequencies for the corresponding adsorbate optimized geometry. However, there are few examples of

theoretical studies for acetonitrile adsorption on Pt. Density functional theory (DFT) calculations by Markovits et al.[17] indicated that the most stable adsorption mode on Pt(111) in UHV conditions is the re-hybridized acetonitrile bonded with the C-N bond parallel to the Pt surface. They also found that on-top adsorption through the N atom is also possible, and a change of the orientation with the methyl group toward the surface was favored when an external electrical field was applied. Pašti et al. also carried out a theoretical study and the same adsorption geometries for acetonitrile on platinum surfaces were proposed.[18] Note that the previous theoretical studies have not considered other possible intermediate species that could be eventually formed during the reversible reduction/oxidation processes of acetonitrile at metal surfaces.

The ORR on polycrystalline Pt and Au in aqueous media with different acetonitrile concentrations was studied for the first time by Srejić et al. in 0.1 M $HClO_4$ as supporting electrolyte.[19] Rotating disk electrode (RDE) measurements pointed out both a displacement of the onset potential to less positive values and a decrease of the limiting current density as acetonitrile concentration was increased. This behavior was attributed to the occupation of a certain fraction of Pt sites by adsorbed acetonitrile which would hinder the adsorption of O_2 as a reactant. Similar inhibiting effects of acetonitrile were observed in sodium chloride electrolyte solutions.[20] ORR in the presence of acetonitrile was also studied using a rotating ring-disk electrode (RRDE)[21] showing that the amount of H_2O_2 as the final product increased in the presence of acetonitrile. The theoretical study by Pašti et al. mentioned above was combined with RDE measurements on polycrystalline Pt in 0.1 M $HClO_4$ and 0.05 M H_2SO_4 solutions with 4×10^{-4} M CH_3CN.[18] These authors also observed a diminution of the current densities on the positive-going scans, but the differences between sulfuric acid and perchloric acid were less important in the presence of acetonitrile. This behavior was

attributed to the suppression of sulfate anion adsorption in the former case.[18] In addition, oxygen reduction current densities in the negative-going direction were increased for both electrolytes in the presence of acetonitrile, probably due to the suppression of surface oxidation. The effect of acetonitrile was also studied in a PEMFC system showing performance losses and changes in current density distribution.[22]

In this work, the adsorption and surface reactivity of acetonitrile on Pt(111) and Pt(100) well-oriented electrode surfaces are first studied by using cyclic voltammetry measurements in 0.1 M $HClO_4$ and 0.1 M NaOH solutions with acetonitrile concentrations ranging from 10^{-3} M to 1 M. The results are complemented with in-situ infrared studies and DFT calculations in order to obtain more information about the nature of the adsorbed species. This detailed study is carried out to solve some inconsistencies that can be found in the previous literature regarding the nature of adsorbed species coming from acetonitrile. For example, the adsorbed intermediate formed after the first one-electron reduction of adsorbed acetonitrile is proposed in [22] to be a species that is adsorbed through the carbon and the adjacent nitrogen with the double bond parallel to the surface, while in the previous work by Morin et al. this intermediate is proposed to have a tilted C-N bond with respect to the metal surface.[9] The theoretical studies carried out to date only considered the initially adsorbed acetonitrile but not the possible adsorbates coming from the latter species. Thus, a detailed fundamental study is necessary to rationalize the previous knowledge. Finally, the effect of acetonitrile toward the ORR in perchloric acid and sodium hydroxide solutions is studied using the hanging meniscus rotating disk electrode (HMRDE) configuration. The use of Pt(111) and Pt(100) electrodes allows the study of the structural effects on the corresponding electrode processes under these conditions.

2. Experimental

Reagents and cleaning procedure. The reagents used for the preparation of the working solutions were concentrated $HClO_4$ (Merck, for analysis), NaOH (Merck, Suprapur, 99.99%), D_2O (Aldrich, 99.9 atom % D) and CH_3CN (Sigma-Aldrich, anhydrous, 99.8%). Ar, H_2, and O_2 (N50, Air Liquide) gases were employed. Ultrapure water (ElgaPureLab Ultra, 18.2 MΩ cm) was used for glassware cleaning and the preparation of the solutions. Glassware was cleaned by soaking in an acidic $KMnO_4$ solution during at least 12 h and then rinsed with a solution of H_2O_2 and H_2SO_4 in ultrapure water to remove traces of manganese oxide. Finally, it was boiled repeatedly in ultrapure water for at least 4 times.

Electrochemical measurements. Cyclic voltammetry experiments were performed in an all-Pyrex three-electrode electrochemical cell following the general procedure described in [23]. Single crystal electrodes with Pt(111) and Pt(100) well-defined orientations were prepared from Pt beads ca. 2 mm in diameter according to the methodology described by Clavilier et al.[24] Working electrodes were flame annealed before each measurement in a propane-oxygen flame and afterward it was cooled in an Ar/H_2 (3:1) atmosphere. Then they were protected with an ultrapure water drop saturated with these gases during its transference to the electrochemical cell. The mentioned cooling atmosphere minimizes the formation of surface oxide thus ensuring that the surface structures agree with those expected for each orientation.[25] The counter electrode was a Pt coiled wire cleaned by flame annealing. The reference electrode was a reversible hydrogen electrode (RHE) in contact with the solution through a Luggin capillary. In this work, all potential values are referred to RHE. The effect of

acetonitrile concentration was studied by successive addition of acetonitrile to the electrochemical cell. In these experiments, the flame-annealing treatment was repeated before each measurement.

An EG&G PARC signal generator and eDAQ EA161 potentiostat with an Edaq e-corder ED401 recording system were used in the (spectro)electrochemical measurements, which were all carried out at room temperature. ORR studies were performed by means of HMRDE measurements using an EDI101 rotating electrode system (Radiometer analytical) in which the platinum single crystal electrodes described above were inserted. Rotation rate was controlled by a Radiometer CTV 101 unit (Radiometer analytical).

Infrared spectroelectrochemical experiments. In-situ external reflection infrared measurements were performed by using a Nexus 8700 (Thermo Scientific) FTIR spectrometer equipped with an MCT-A detector and a Veemax (Pike Tech.) The glass spectroelectrochemical cell was coupled to a prismatic CaF_2 window beveled at 60° and contains a Pt counter electrode and an RHE as reference electrode. All the spectra were collected with 8 cm^{-1} resolution and are presented in absorbance units (a. u.) as – log (R/R_0), where R and R_0 represent the single beam sample and reference reflectivity spectra, respectively. Therefore, positive-going and negative-going bands correspond, respectively, to the formation and consumption of species for the sample spectrum with respect to the reference spectrum. Sets of 100 interferograms were obtained at different sample potentials and referred to a single beam reference spectrum collected in the acetonitrile-containing solution at the indicated reference potential (E_{ref}). Experiments were performed both in H_2O and D_2O as solvents. Deuterium oxide was used in order to avoid spectral interferences from OH bending modes of water around 1600 cm^{-1}.

3. Computational details

Geometry optimization and harmonic frequency calculations were carried out for acetonitrile and related species adsorbed on periodic models for the Pt(111) surface. All calculations were done within the DFT-GGA approach of Perdew, Burke and Ernzehof [26,27] as implemented in the VASP code,[28-31] using the Projector-Augmented-Wave method,[32,33] and a cutoff energy value of 400 eV.

The simulation cells contained a slab formed by 4 metallic layers (with 9 Pt atoms each), with a (3x3) surface periodicity, for a total of 36 metal atoms. A vacuum region of more than 1.2 nm was included to avoid any significant coupling between the adsorbate species and the back side of the slab. The positions of the metal atoms were kept fixed, with a nearest-neighbor distance of 0.28171 nm obtained from the fitting of the calculated bulk energy-vs-bulk volume curve to a Murnaghan equation of state.

Sampling of the k-points in the first Brillouin zone used an automatic Monkhorst-Pack [34] (3x3x1) scheme. The second order Methfessel-Paxton[35] smearing method was used with $\sigma = 0.1$ eV. The convergence criteria used were 10^{-5} eV for the electronic energy, and forces on atoms below 0.02 eV/Angstrom, for the geometry optimization (without restrictions) of the molecular adspecies. The calculated vibrational frequencies were obtained using the harmonic approximation, with atomic displacements of 0.02 Angstrom for each coordinate. The calculated frequency values, which are reported unscaled, have relative errors lower than 2-3% of the calculated frequency, as estimated from previous works.[36,37] For all the calculations reported here, the (3x3) simulation cell contained only one adsorbate species on one side of the slab. This situation corresponds to the low coverage limit ($\theta = 1/9$), where lateral interactions

between adsorbate replicas are expected to be minimal, almost negligible. Optimized geometries and vibrational modes were visualized using Molden[38] and Jmol.[39]

4. Results and discussion

4.1. Characterization of the electrochemical interface in the presence of acetonitrile

4.1.1. Voltammetric measurements

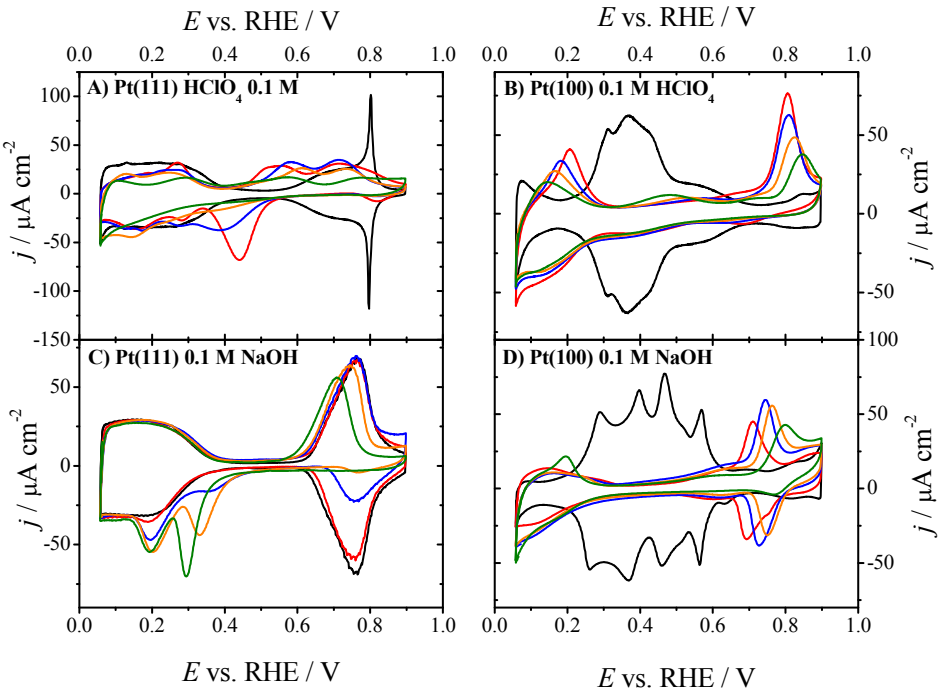

Figure 1. Voltammetric profiles for (A,C) Pt(111) and (B,D) Pt(100) in (A,B) 0.1 M $HClO_4$ and (C,D) 0.1 M NaOH in the absence of acetonitrile and with different concentrations from 10^{-3} M to 1 M. Black line: Without acetonitrile; red line: 10^{-3} M CH_3CN; blue line: 10^{-2} M CH_3CN; purple line: 0.1 M CH_3CN; green line: 1 M CH_3CN. Scan rate: 50 mV s^{-1}.

The metal|electrolyte interfaces for Pt(111) and Pt(100) were characterized by means of cyclic voltammetry in both acidic and alkaline solutions containing different concentrations of acetonitrile ranging from 10^{-3} M to 1 M. Figure 1 shows the stationary voltammograms obtained under these conditions for Pt(111) (A, C) and Pt(100) (B, D) in 0.1 M $HClO_4$ (A, B) and 0.1 M NaOH (C, D). Results in 0.1 M $HClO_4$ for the lowest concentration of acetonitrile are in agreement with the previous work by Morin et al.[8,9]

and clearly point out that acetonitrile adsorption and its surface redox processes are structure sensitive.

For the Pt(100) electrode in acidic solutions, it can be observed that hydrogen adsorption/desorption region is practically blocked since no signals are observed between 0.3 and 0.7 V, in contrast with the observed behavior for the Pt(111) surface where these states are only blocked to a low extent. Additionally, several redox processes associated with the adsorbed acetonitrile molecules are clearly visible. For Pt(100) in acidic solutions, two anodic peaks appear below 0.30 V and above 0.70 V with ill-developed cathodic counterparts, especially that above 0.70 V. In this case, current densities decrease as acetonitrile concentration is increased possibly due to oligomerization processes in the adlayer.[8] The shape of the corresponding voltammetric features is very dependent both on the acetonitrile concentration and, for a given concentration, on the exact potential limits of the voltammetric scan.

The effect of the polarization range on the shape of the cyclic voltammograms is especially remarkable for Pt(111) in 0.1 M $HClO_4$ (Figure 2). Fig. 2A shows the voltammetric profiles obtained for Pt(111) in a 0.1 M $HClO_4$ + 10^{-3} M CH_3CN solution for two different upper potential limits (E_u), namely 0.58 and 0.90 V. From the diminution of the charge related to hydrogen adsorption on the Pt(111) electrode when acetonitrile is present in solution, it is clear that acetonitrile species are initially adsorbed at low potentials. When the electrode is cycled between 0.06 and 0.58 V, only two reversible peaks, *a1* and *c1*, can be observed at ca. 0.55 V. However, if E_u is increased up to 0.9 V, the voltammogram in the region between 0.4-0.6 V is modified and a sharp reduction peak *c2* centered at ca. 0.45 V appears with a related anodic peak *a2* at ca. 0.50 V. Besides, peak *a1* slightly decreases and shifts to less positive potentials and reduction peak *c1* disappears completely. In addition, oxidation and reduction peaks

a3 and *c3* can be observed at high potentials. It is important to remark that although c*2* and *a2* (together with *a1)* were initially attributed to the first stage of the reduction and re-oxidation of acetonitrile adsorbed species,[8] these peaks only appear when the upper limit is higher than 0.60 V. Therefore, some reaction is taking place above this potential, which alters the nature of the adsorbed species and gives rise to a new redox feature associated with peaks *a2* and *c2*.

Using all this information and the comparison with previous results an explanation for these redox phenomena can be given. The reversible pair of peaks *a1* and *c1* are similar to those observed in the presence of adsorbed cyanide on Pt(111) electrodes,[40] which are related to the OH adsorption/desorption processes on the free platinum sites modified by the presence of neighboring adsorbed species. Thus, these peaks can be assigned to the adsorption/desorption of OH on free sites close to adsorbed acetonitrile-related species. Then, peaks *c2* and *a2* should be attributed to the reduction and re-oxidation of some acetonitrile-related adsorbates which only can be formed at potentials higher than 0.60 V. This oxidation/reduction processes in the acetonitrile layer should affect the OH adsorption, and for this reason, alters the process of OH adsorption/desorption of peaks *a1* and *c1*. Peaks *a3* and *c3* would arise from a second stage of OH adsorption/desorption. The intensity of peak *c3* is much lower than that of peak *a3*, suggesting that a fraction of OH species are consumed in some surfaces processes which take place at these potentials and hence much fewer hydroxyl anions are desorbed in the negative-going scan. In parallel, it has to be noted that peak *c2* has a larger charge than peak *a2*, indicating that the corresponding processes are not totally reversible.

The evolution of the voltammetric profiles after reaching progressively higher potentials by a stepwise increase of the upper potential limit in consecutive cycles will

shed some additional light into these processes (Fig. 2B). As can be seen, peak *c1* disappears gradually accompanied by the appearance of peaks *c2* and *a2*. In conclusion, the higher the upper potential limit, the higher the fraction of adsorbed species which are reduced at 0.45 V in peak *c2*. It can be noted that the small cathodic peak *c4* at ca. 0.27 V is also related to the processes that take place at high potentials. Additionally, when the electrode is immersed in the acetonitrile-containing solution at 0.10 V, the second cycle recorded up to 0.9 V is different from the first one (Fig. S1). Besides the change of the oxidation wave between 0.50 V and 0.60 V (in agreement with the behavior described above), the peak *a3* becomes less intense and moves slightly to a more positive potential. This also suggests that some processes occur at potentials beyond 0.65 V that change the state of adsorbed acetonitrile.

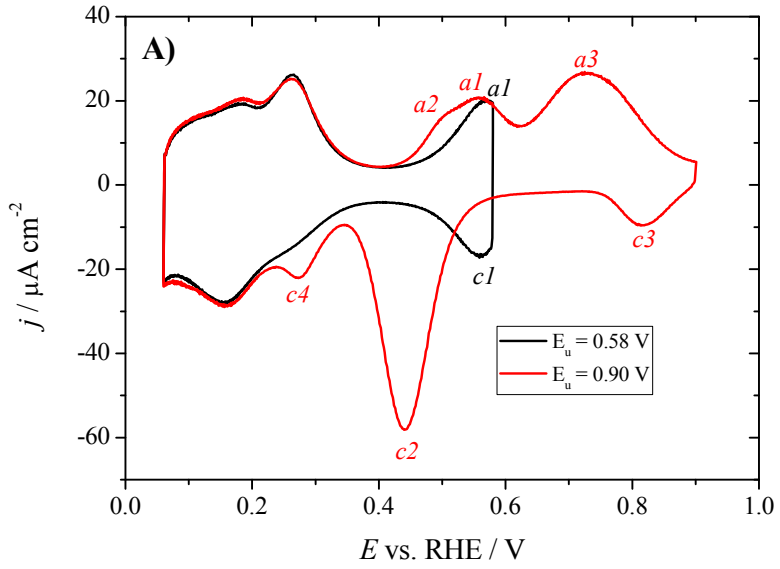

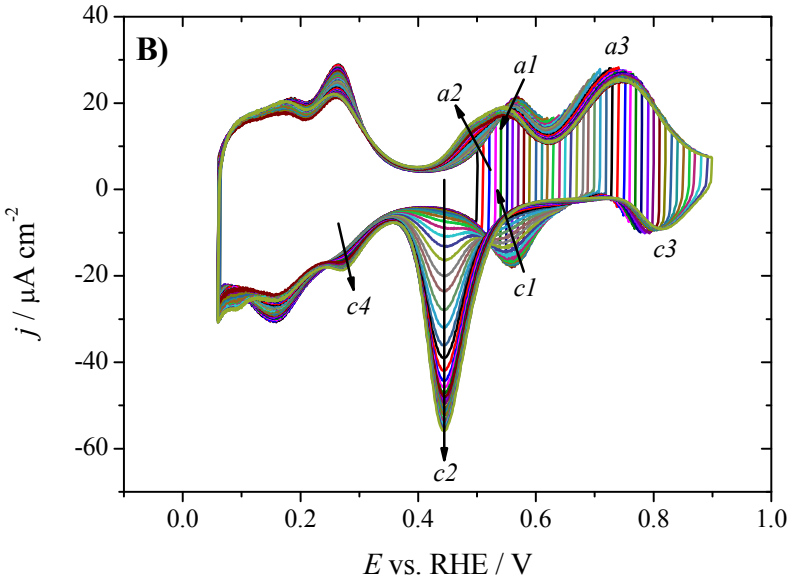

Figure 2. Voltammetric profiles recorded for Pt(111) in 0.1 M $HClO_4$+ 10^{-3} M CH_3CN with E_u = 0.58 V and 0.90 V (A) and progressively increasing E_u by 0.01 V steps from 0.50 V to 0.90 V (B). Scan rate: 50 mV s^{-1}.

The effect on the CV of a variation of the lower potential limit (E_l) was also analyzed (Fig. 3A). When E_l is fixed at 0.36 V, the peak *a2* is more pronounced and peak *a1* is almost negligible. For more positive E_l values, peak *a2* becomes sharper and peak *a1* disappears completely. It can also be appreciated that the intensity for peak *a3* diminishes as the lower potential is made more positive. In addition, peaks *a2* and c2 disappear progressively upon continuous potential cycling between 0.40 and 0.63 V after a potential excursion to high potentials (Fig. 3B). Another remarkable observation is that, when the electrode is immersed at 0.8 V before performing the cyclic voltammetry measurements, the charge under peaks *a3* and *c3* slightly diminishes, the reduction peak *c2* becomes more intense and additional reduction currents can be observed at potentials lower than 0.20 V (Fig. S2).

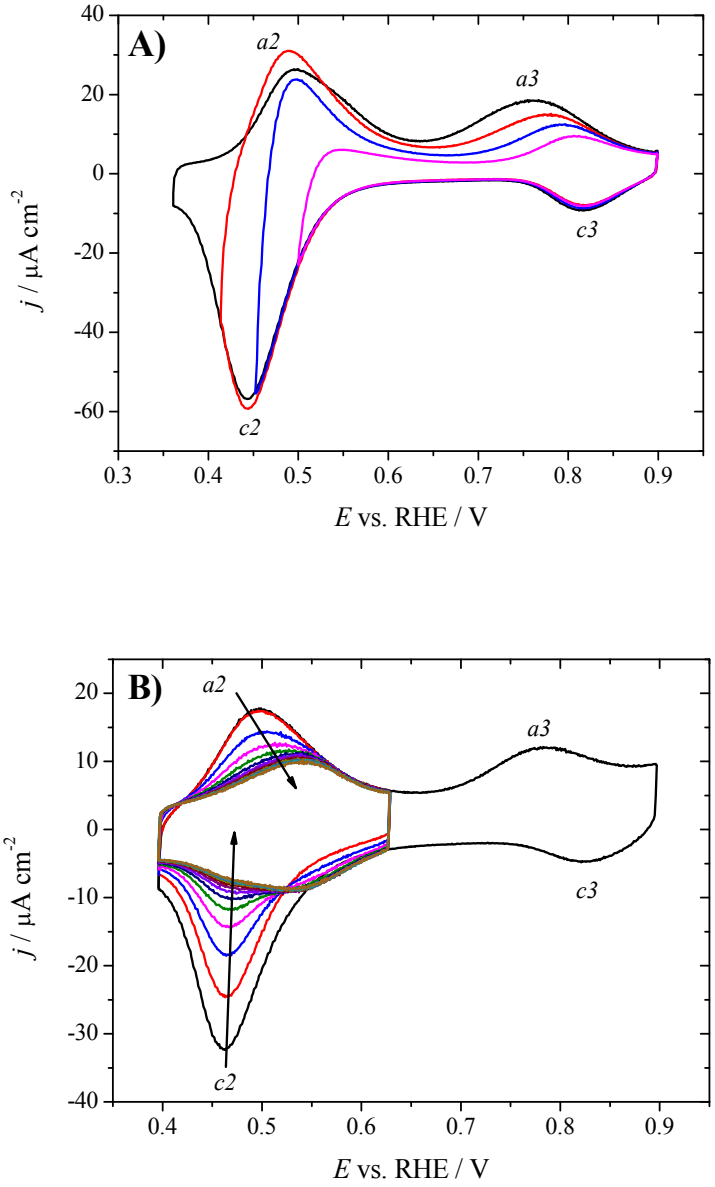

Figure 3. A) Voltammetric profiles for Pt(111) in 0.1 M $HClO_4$ + 10^{-3} M CH_3CN with E_u = 0.90 V and different E_l down to 0.36 V. (B) Several cycles with E_l = 0.40 V and E_u = 0.63 V after a potential excursion up to 0.90 V. Scan rate: 50 mV s^{-1}.

All these results suggest that adsorbed acetonitrile undergoes some chemical surface reaction with adsorbed OH to form an adsorbed intermediate which is reduced around 0.45 V, with peak *a2* corresponding to the re-oxidation of this intermediate. This would explain the drastic diminution of signals *a3* and *c3* when the electrode is immersed at 0.8 V and the appearance of peak *c2* only after high potentials are reached. The decrease in the intensity of peaks *a2* and *c2* in Fig. 3B probably arises from the fact

that the species giving rise to peak *c2* are only formed at potentials higher than 0.65 V. If the potential remains below 0.65 V, this species is not formed and peaks *a2* and *c2* are not restored. The sharpening of peak *a2* and the decrease of intensity of peak *a1* when E_l is fixed at more positive potentials can be also explained by this mechanism. The additional currents observed below 0.2 V in Fig. S2 (when the electrode is polarized at high potentials) could be due to a further reduction of the resulting adsorbed species, which would desorb from the electrode, thus returning to the stationary state. In-situ infrared measurements and DFT calculations results will be presented in sections 4.1.2 and 4.1.3, respectively, in order to clarify the nature of the possible intermediate species formed in these processes.

Regarding the acetonitrile concentration effect shown in Figure 1A, the intensity of peak *c2* for Pt(111) in 0.1 M $HClO_4$ decreases as acetonitrile concentration is increased and its potential moves to less positive values. This is because the coverage of acetonitrile-related adsorbed species increases, making more difficult the reduction step, despite the fact that currents in the hydrogen adsorption/desorption region are not largely diminished. The peaks at high potentials are also modified: peak *a2* moves to more positive potentials since the re-oxidation of the intermediate is also more hindered at higher coverage, and peaks *a3* and *c3* decrease their intensity for high concentrations of acetonitrile since there are less available sites for hydroxyl anions adsorption.

The characterization of acetonitrile adsorption on Pt(111) and Pt(100) in alkaline media is presented for the first time in Fig. 1C and 1D, respectively. For Pt(111) and 10^{-3} M CH_3CN, only a slight diminution of the OH desorption peak and a small cathodic peak are observed at 0.20 V. This fact clearly indicates that the amount of adsorbed acetonitrile for this concentration is very low. As acetonitrile concentration is increased several effects are observed in the voltammogram. First, the OH desorption

signal decreases drastically until it disappears completely for 1 M CH_3CN. Secondly, the peak at 0.20 V increases its intensity and another peak is developed between 0.30 and 0.40 V, being more intense for the highest concentration of acetonitrile. It is important to highlight that the hydrogen adsorption/desorption feature remains practically unchanged for all acetonitrile concentrations. This means that, at low potentials, the surface coverage of adsorbed acetonitrile is negligible. From the observed voltammetric profiles in Figure 1C, a similar behavior to the case of 0.1 M $HClO_4$ can be proposed: adsorbed intermediates could be formed at high potentials by surface chemical reaction between adsorbed acetonitrile and adsorbed OH. In the 0.1 M NaOH solution, these species are desorbed upon reduction at low potentials. Therefore, in alkaline conditions, the coverage of adsorbed species at low potentials would be much lower than in acid media. However, in-situ infrared measurements in basic media presented in Section 4.1.2 will corroborate the presence of adsorbed acetonitrile at low potentials.

For Pt(100) the most noticeable features in acetonitrile-containing alkaline solutions are the pair of anodic and cathodic peaks that appear at ca. 0.7 V (Figure 1D). Both peaks undergo shifting to more positive potentials as acetonitrile concentration is increased. The origin of these peaks could be the adsorption/desorption of hydroxyl anions modified by the presence of acetonitrile adsorbed species.

4.1.2. In-situ infrared experiments

In-situ FT-IR experiments were carried out in order to identify the adsorbed species formed from acetonitrile both in $HClO_4$ and in NaOH solutions. Fig.4 shows the obtained spectra for Pt(111) in 0.1 M $HClO_4$ + 10^{-2} M CH_3CN, using either H_2O (A) or D_2O (B) as solvent. In each panel, the upper set of spectra was collected by decreasing

the electrode potential after immersion at 0.90 V. These spectra are referred to the single beam spectrum collected at 0.90 V. Regarding the lower set of spectra, which were collected in a separate experiment, immersion potential was 0.10 V. When water is used as solvent, the possible observable bands around 1600 cm^{-1} are masked by the overlapping with the bands of the bending modes of H_2O. No clear features are observed around 1600 cm^{-1} in the spectra reported in Fig. 4A, which shows two bands at ca. 1452 and 1375 cm^{-1}. These bands are negative when 0.90 V is selected as the reference potential (upper set of spectra) and positive when the reference potential is 0.10 V (lower set). This means that the species responsible for these bands are consumed when decreasing the electrode potential from 0.90 V to 0.10 V.

When deuterium oxide is used as solvent (Figure 4B), a new band centered at 1635 cm^{-1} is clearly observed. Since the spectral interferences from the OH bending mode of water have been removed under these conditions, the observed feature must be related now to acetonitrile species. As this band is positive when the reference spectrum is chosen at 0.90 V and becomes more intense as the electrode potential is decreased, the responsible species are generated in the negative-going scan. As previously observed by Morin et al [9], a negative band around 1404 cm^{-1} is observed in this latter solvent, which could be related to the bands observed at 1452 and 1375 cm^{-1} in H_2O.

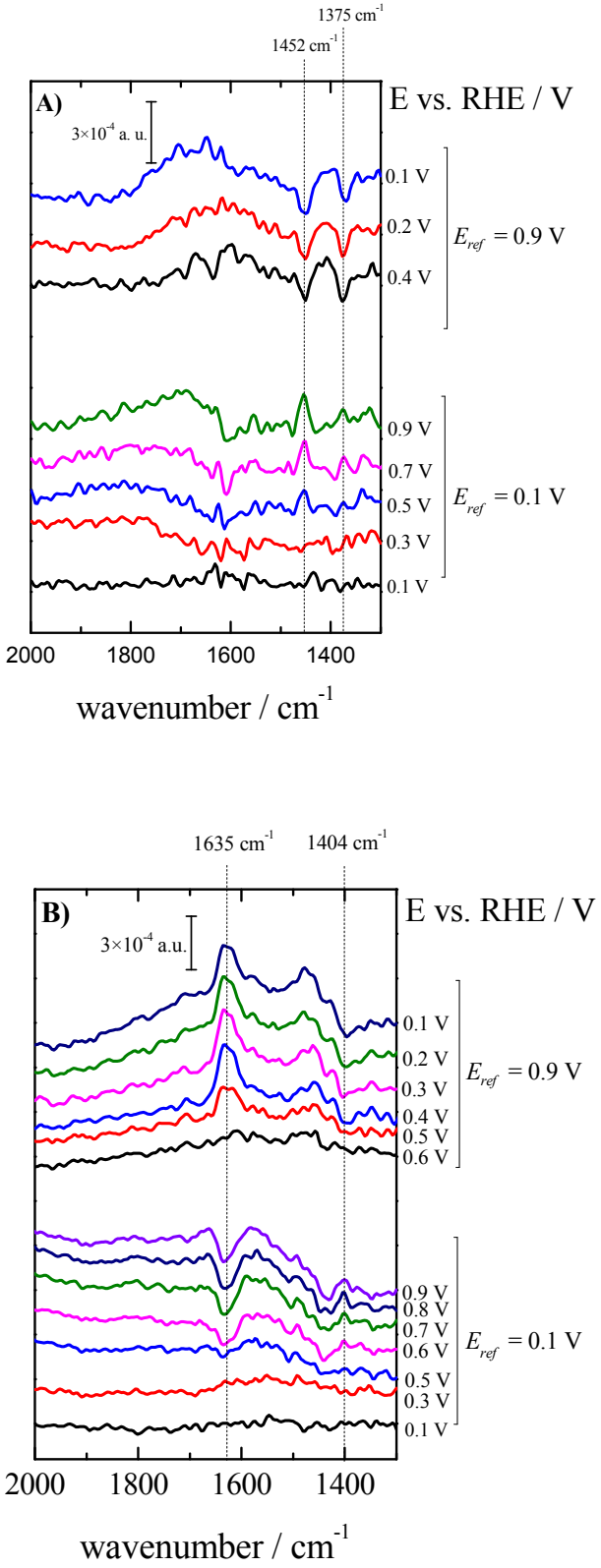

Figure 4. In-situ FT-IR spectra for Pt(111) in 0.1 M $HClO_4$ + 10^{-2} M CH_3CN using H_2O (A) and D_2O (B) as solvents; number of interferograms: 100; resolution: 8 cm^{-1}. The working electrode was flame-annealed and cooled in Ar/H_2 3:1 atmosphere for each set of spectra at different E_{ref}.

The spectroscopic results presented above are in agreement with those reported by Morin et al. [9]. They also observed the band at 1635 cm^{-1} at low potentials and assigned it to a reduced intermediate species formed from adsorbed acetonitrile. This reduced species would have a C=N double bond tilted with respect to the surface. Hence, and according to the surface selection rule for adsorbed species at metal surfaces [40], its stretching vibration mode would be infrared-active. These authors justified the observed band frequency value on the basis of both the frequency values reported in the literature for C=N bonds in iron coordination complexes and on the spectra reported for acetonitrile chemisorbed on Pt(111) under UHV conditions.[9,11,12] According to Morin *et al.,*[9] the band at ca. 1410 cm^{-1} for CH_3CN in D_2O solutions would be related to the bending of the methyl group. The observation of this feature at high potentials, for which the band at ca. 1635 cm^{-1} is not observed, would be linked to the reorientation of the C=N bond from a tilted orientation (infrared active) at a low potential to parallel to the surface at high potentials (infrared inactive). This change in the acetonitrile orientation would also change the contribution of the methyl group to the absorption band at ca. 0.50 V, giving rise to a consumption band at 1404 cm^{-1} when the potential is changed from higher to lower potentials. In section 4.1.3, results from DFT calculations for acetonitrile and other related adsorbates will be presented as to provide a sound basis for the elucidation of the nature of the adsorbates as well as for band assignments.

Results shown in Fig. 5 for Pt(100) were obtained in a 0.1 M $HClO_4$ solution in D_2O in an experiment in which the electrode was immersed in the acetonitrile-containing solution at 0.85 V and then the electrode potential changed to less positive values. The same bands as for Pt(111) are observed but with a less positive onset potential, which is in agreement with the voltammetric profiles shown in Figure 1B that exhibit reduction currents below 0.30 V. However, at 0.10 V the band intensities are

similar for Pt(111) and Pt(100) electrodes, unlike the results reported in ref. [9], showing much less intense bands for Pt(100). The infrared spectra presented here corroborate that the acetonitrile coverage on Pt(100) can be similar or even higher than in Pt(111), as also pointed out by cyclic voltammetry results. The reason for such a low intensity for the bands in the case of Pt(100) in ref. [9] could be due to a lower quality of the electrodes in comparison with those used in the present work.

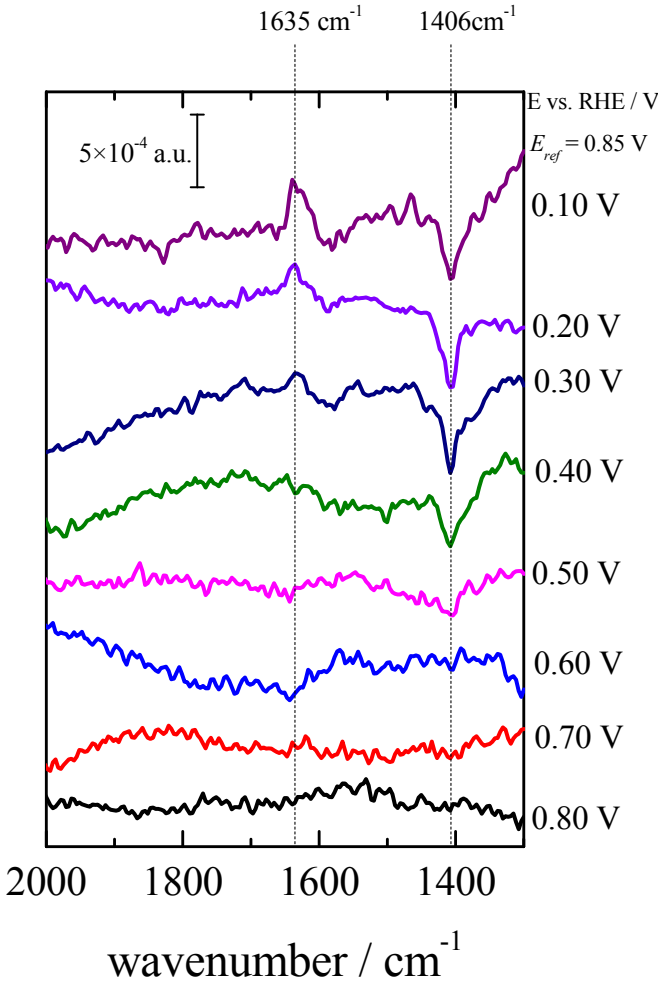

Figure 5. In-situ FT-IR spectra for Pt(100) in 0.1 M $HClO_4$ + 10^{-2} M CH_3CN using D_2O as solvent; E_{ref}: 0.85 V; number of interferograms: 100; resolution: 8 cm^{-1}.

In situ infrared experiments for Pt(111) in 0.1 M NaOH using D_2O as the solvent were also performed for the first time. The corresponding spectra, collected in a similar

way as those shown in Figure 4, are reported in Figure 6. In this case, a 0.1 M acetonitrile concentration was used in order to clearly see the spectral features, since for 10^{-2} M CH_3CN no bands were observed. Analogous bands to those reported in acidic media are observed. Namely, and for a reference potential of 0.90 V, a positive band centered at 1633 cm^{-1} appears in the spectra recorded from 0.60 to 0.10 V whereas a negative band at 1403 cm^{-1} can be observed in the same potential region. It is important to remark that these bands are also observed with opposite sign when the reference potential is 0.10 V. From these data, the nature of the intermediates seems to be similar to those in 0.1 M $HClO_4$. This indicates that, although the coverage of acetonitrile adsorbed species at low potentials is much lower than in acidic media as deduced from the cyclic voltammetry results, some species are still present on the electrode surface since infrared bands can be observed (but at higher acetonitrile concentrations than in the case of acidic solutions).

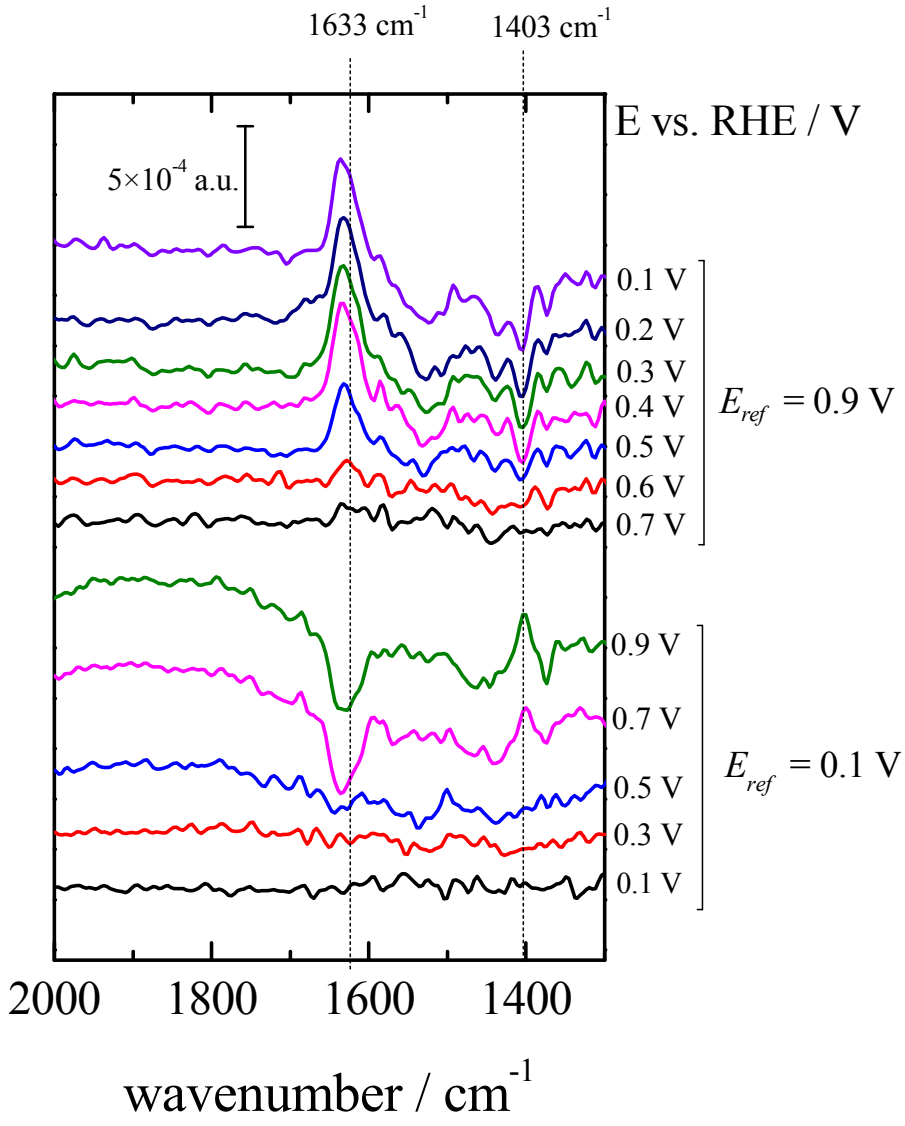

Figure 6. In-situ FT-IR spectra for Pt(111) in 0.1 M NaOH + 0.1 M CH_3CN using D_2O as solvent; number of interferograms: 100; resolution: 8 cm^{-1}. The working electrode was flame-annealed and cooled in Ar/H_2 3:1 atmosphere for each set of spectra at different E_{ref}.

4.1.3. Density functional theory (DFT) calculations

In order to obtain information about adsorption geometry and vibrational frequencies of adsorbates that could be formed from acetonitrile, either by reduction (hydrogenation) or hydroxylation, we have studied a number of possible molecular configurations for each of the more likely species, on a model Pt(111) surface. Calculations for acetonitrile-related adsorbates at Pt(100) surface are out of the scope of

this work. However, since the experimental potential-dependent infrared spectra reported above are similar for both Pt(111) and Pt(100) electrodes, it could be assumed in a first approximation that similar species are formed irrespective of the surface orientation. Figure 7 shows the optimized geometries obtained for acetonitrile C_2H_3N (species A), reduced species with formulae C_2H_4N (species B, C) and C_2H_5N (species D, E), and hydroxylated species with formulae C_2H_4NO (species F) and C_2H_5NO (species G, H).

In the case of adsorbed acetonitrile (A), the optimized structure agrees with that reported in previous DFT studies.[17,18] The geometrical parameters are consistent with sp^2 hybridization of both atoms (C and N) bonded to the metal, in which the CCN plane is essentially perpendicular to the metal surface. In this configuration, the CN bond is almost parallel to the metal surface, with each of both atoms being monocoordinated to one surface Pt atom, in near-on-top positions. The orientation of the CN bond makes impossible the experimental detection of its stretching mode using surface vibrational spectroscopy, as a consequence of the surface selection rule. This rule requires the existence of a non-zero component normal to the surface of the transition dipole moment for the transition to be observable.[41]

Optimized structures B and C correspond to species that can be reductively formed from adsorbed acetonitrile after a monoelectronic step with the incorporation of a hydrogen atom. In structure B, the added hydrogen atom is bonded to the nitrogen atom. The overall structure closely resembles that of the species A (rehybridized acetonitrile). In the case of structure C, where the additional hydrogen is bonded to the carbon atom (now with sp^3 geometry), the nitrogen sits on a three-fold hollow site. This latter structure is, in any case, significantly less stable than structure B by around 65 kJ mol^{-1} (all relative energies are given without including the zero-point vibrational

energy correction). As this energy difference is substantially higher than the average thermal energy per molecule at room temperature (less than 3 kJ mol^{-1}), we can discard this species for the band frequency assignments. Moreover, for species C, the orientation of the NCC molecular plane, and of the Pt-N bond, both being perpendicular to the metal surface, would make possible the experimental observation of the CN stretch, as this bond deviates from the surface normal by around 52º.

The additional incorporation of a second hydrogen atom either to the C or N atom not previously hydrogenated produces species with C_2H_5N stoichiometry. The optimized structure D is bonded to the metal in a monodentate configuration through the nitrogen atom, located on top of a surface Pt atom, while the geometry of structure E is close to that of species C, with an additional hydrogen atom. However, the additional NH bond in E involves the change of the metal-nitrogen coordination from the 3-fold hollow to a two-fold bridge site. This latter species is less stable than the monocoordinated one (D), by around 35 kJ mol^{-1}. This difference is sufficiently high as to make this structure unlikely to appear at room temperature.

The oxidized structures studied were restricted to those with the hydroxyl group bonded to the nitrogen atom, forming oxime moieties, such as in adspecies F and G, or as a dehydrogenated (in the N atom) hydroxylamine (species H). The oxime F, which differs from acetonitrile in the added OH group, keeps the CN double bond parallel to the surface, making impossible the observation of the corresponding stretching mode in the in-situ IR experiments. Hydroxylation at the carbon atom instead would give rise to less stable species, as this would imply the 3-fold hollow coordination of the nitrogen (vide supra for the hydrogenated species). Structures G and H are the result of the addition of one water molecule to the double bond of adsorbed rehybridized acetonitrile, and its formation under the electrochemical conditions can involve electrochemical as

well as chemical steps. For both structures, the hydroxyl group is bonded to the nitrogen atom, with the unidentate configuration (species G) being 39 kJ mol^{-1}more stable than the bidentate one (H).

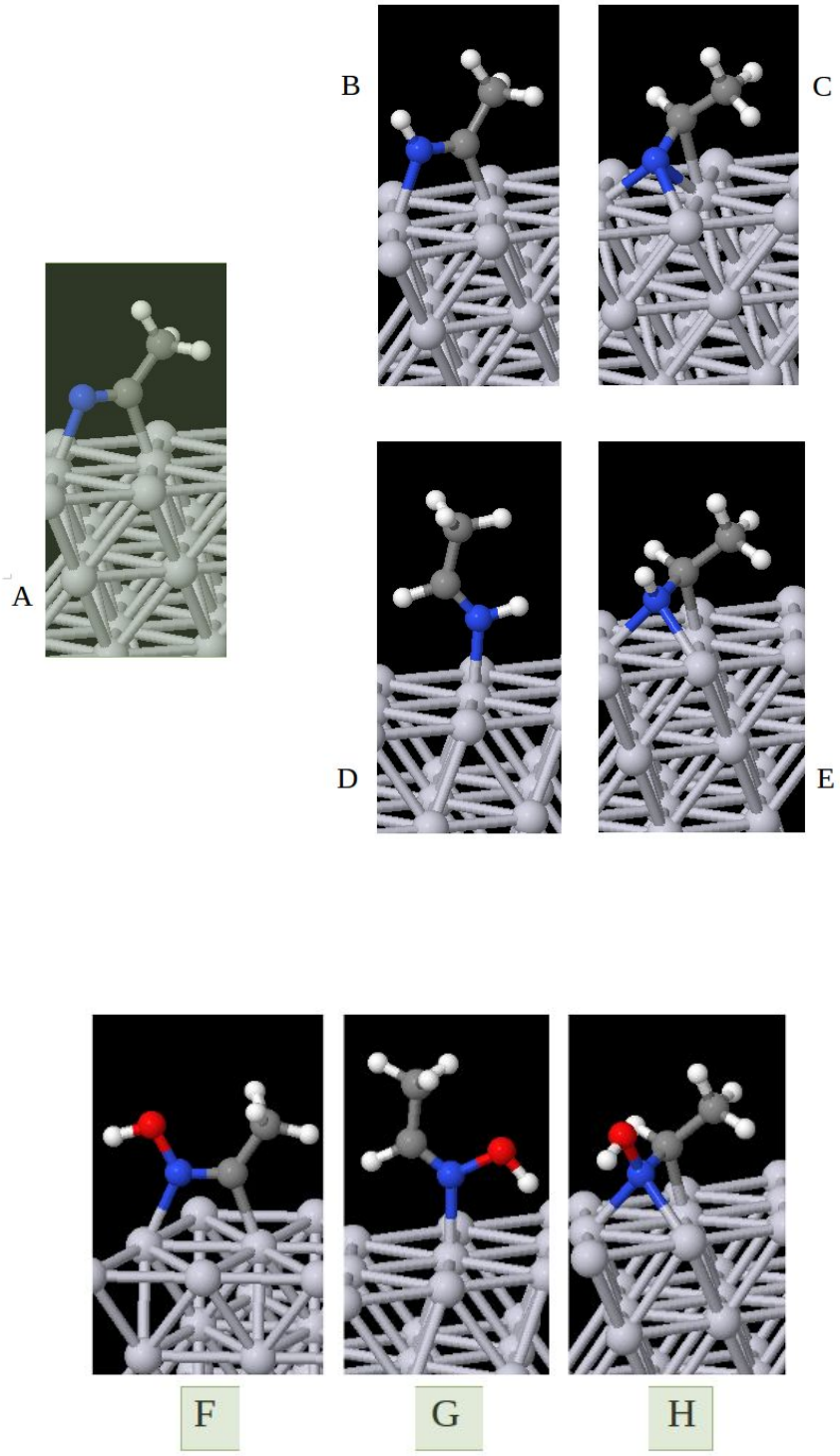

Figure 7. Optimized adsorption geometries of acetonitrile (A), monohydrogenated acetonitrile (B, C), dihydrogenated acetonitrile (D, E), and hydroxylated acetonitrile derivatives (F, G, H) on a model Pt(111) surface.

From the optimized geometries discussed above, the harmonic vibrational frequencies were calculated (see Tables 1 and 2) for species A to H, corresponding to formulae CH_3CN, C_2H_4DN, $C_2H_3D_2N$, C_2H_3DNO, and $C_2H_3D_2NO$. These are the stoichiometries expected for the hydrogenation and hydroxylation products of acetonitrile when incorporating atoms from deuterated water as the solvent. In all cases, the methyl group has been kept non-deuterated, as it is well known that alkyl groups do not easily exchange protons with the solvent.

The main spectroelectrochemical experimental observations to be explained are the observation of IR absorption band around 1635 cm^{-1} by adspecies present below 0.60 V, and absorption in the range 1300-1500 cm^{-1}, namely around 1452 and 1375 cm^{-1} using H_2O as solvent and ca. 1404 cm^{-1} using D_2O, at potentials above 0.60 V (see previous section). In the following, we will focus mainly on the analysis of the spectra collected in D_2O solutions, since the latter allow a better observation of the band at ca. 1635 cm^{-1}. As stated above, working with non-deuterated acetonitrile (CH_3CN) in D_2O solutions does not imply H-D exchange for the methyl group. Besides, it can be recalled here that the band at ca. 1404 cm^{-1} was observed by Morin et al.[9] in D_2O solutions both for CH_3CN and CD_3CN-containing solutions. In our analysis, we will consider the theoretical frequencies corresponding to the experimental range (from 1300 to 2000 cm^{-1}), which is limited for the lower wavenumbers by the cutoff of the CaF_2 window and, for the higher wavenumbers, by uncompensated bands for the O-D stretching modes of D_2O. Additionally, from the relative stabilities of isomeric species, we can discard species C, E and H (whose calculated harmonic frequencies are also reported in Tables 1 and 2) for the assignment of the experimental frequencies, because those species are not expected to occur at room temperature.

The experimental observation of absorption around 1600-1650 cm^{-1}, typical of double CN bonds, could only be due to adsorbed acetonitrile (A), CH_3-CD=ND (D), or CH_3CD=NOD (G), species which have calculated frequencies at 1644, 1621 and 1616 cm^{-1}, respectively. The surface selection rule, which requires a non-zero component of the transition dipole moment in the direction normal to the metal surface, allows us to discard rehybridized adsorbed acetonitrile (A) as the species responsible for the 1635 cm^{-1} band. It should be noted that the absence of experimental signals in the range 1500-1600 cm^{-1}, where the bands for the CN stretching bands of species B and F are expected to appear, does not allow to rule out their presence at the surface. As in the case of acetonitrile (A), these bands would not be observable as a consequence of the surface selection rule, as the C=N bond is parallel to the surface.

The calculated frequencies for the bending of the methyl group for all the studied species are rather similar. Note that two asymmetric modes appear at ca. 1410-1400 cm^{-1}, whereas symmetric CH_3 bending mode has a lower calculated frequency (namely, between 1350 and 1330 cm^{-1}). On the basis of these frequencies, the pair of asymmetric CH_3 bending modes (which are indistinguishable under the present experimental conditions and appear at significantly lower wavenumbers in the case of the CD_3 group) would explain the experimental bands at ca. 1405 cm^{-1} appearing at potentials above 0.60 V (using 0.10 V as reference potential). Since these bands are totally absent (within the detection limits) at potentials below 0.60 V, where the presence of species D and G has been assumed to exist in order to explain the observation of the C-N stretching band (see above), it has to be considered that the asymmetric CH_3 bending modes are infrared inactive for the latter species. In particular, for species D and G, the orientation of the CC bond is very close to the surface normal, which means that the atomic movements, and in turn, the main contribution to the

transition dipole of the methyl bending mode, are essentially parallel to the surface. This means, taking into account the surface selection rule, that they cannot be detected in our IR experiments. On the contrary, species A, F and B, for which the C-C axis is tilted with respect to the metal surface, could contribute to the absorption in the asymmetric CH_3 bending region for potentials higher than 0.60 V. This would explain the lower absorption around 1400 cm^{-1} in the lower potential range when compared to that from species adsorbed at higher potentials, thus giving rise to negative bands when the spectrum collected at 0.90 V is taken as the reference spectrum. The absence of net absorption in the methyl bending spectral region would rule out the presence of species B (for which a stronger absorption for the methyl bending would be expected) below 0.60 V. It would be difficult to decide on the presence of species B at more positive potentials since its contribution to the observed methyl band would be mixed with that from other adspecies. On the same basis, the presence of some amount of adsorbed rehybridized acetonitrile above 0.60 V cannot be excluded, as the vibrational frequencies of its modes involving methyl bending movements are similar to those of the other species considered.

In the latter analysis, we have not discussed the possible origin of the bands observed at ca. 1452 and 1375 cm^{-1} in water solutions. Note that these frequency values do not seem to fit with the calculated frequencies for asymmetric (1400-1410 cm^{-1}) or symmetric (1350 cm^{-1}) for all the considered species. Morin et al.[9] suggested that these features could be partially related to changes in the interfacial anion/acetonitrile or solvent/acetonitrile structures. DFT calculations including a number of water molecules to check this hypothesis give rise to much more complicated adlayers and make calculations much more time-consuming. This kind of study, as well as that of the eventual effect of adsorbate coverages, is out of the scope of this paper.

From all the data discussed above, a simple explanation for the experimental infrared data could be given based on a potential-dependent interconversion of the proposed species (reactions (3) to (7) of Figure 8). In this way, the conversion of adsorbed acetonitrile (A) into hydroxylated acetonitrile (species F) could be proposed to take place at potentials above 0.60 V. This transformation could in principle proceed either in a direct monoelectronic electrochemical step with consumption of a water molecule and the release of a proton, or via a Langmuir-Hinshelwood type surface chemical reaction between acetonitrile and adsorbed OH (formed in a previous electrochemical step) (reaction (4)). This hydroxylated species could be subsequently reduced at lower potentials. Different possibilities exist, but from the observed bands, the reduction would lead to species G (by incorporating one hydrogen in a monoelectronic electrochemical step, reaction (5)), or D (this would imply the reduction of the hydroxyl in the oxime group) (reaction (7)). Species G could be re-oxidized at E > 0.35 V (reaction 6).

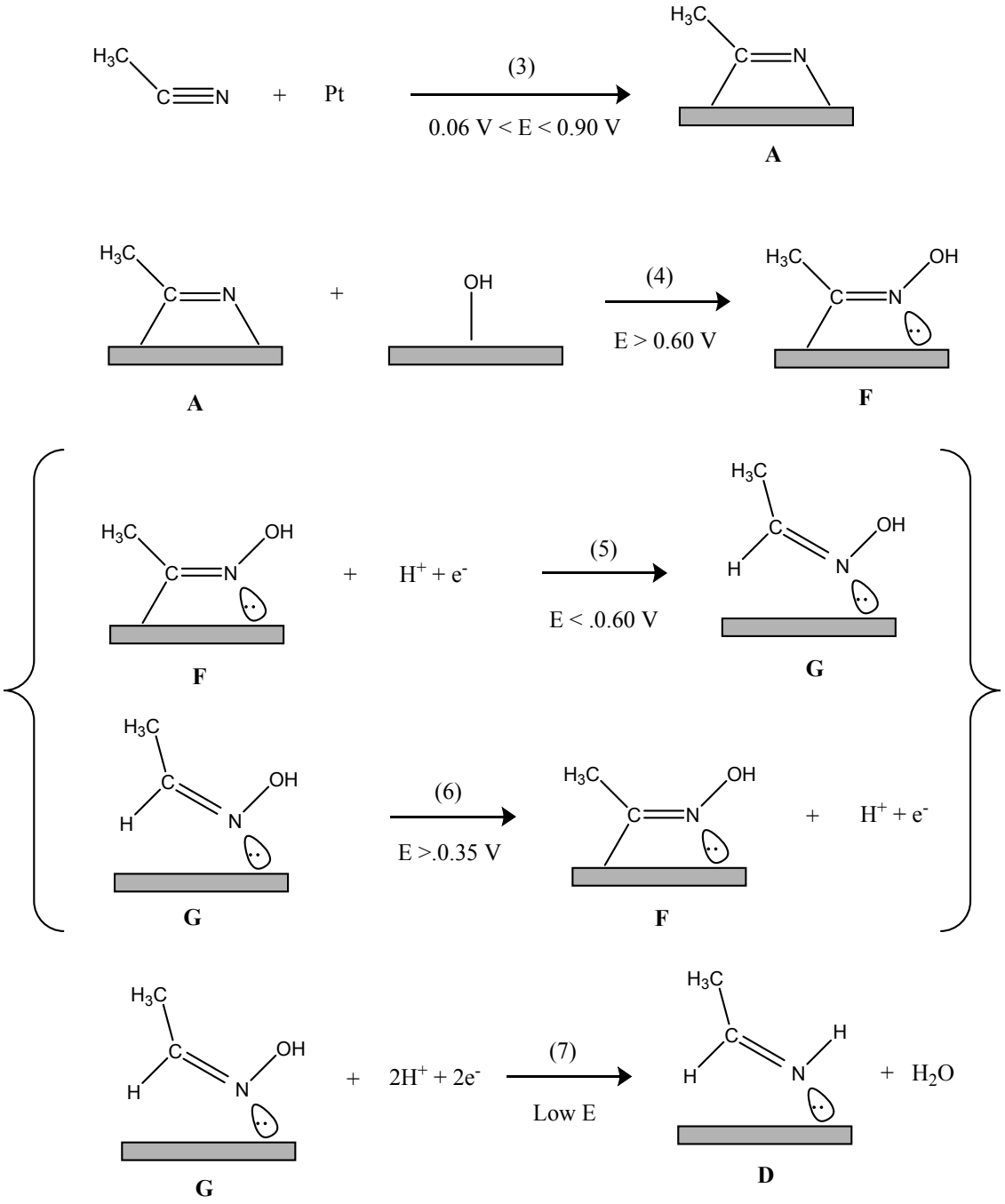

Figure 8. Scheme of the proposed reactions for the adsorption and surface reactivity of CH_3CN on Pt(111).

Table 1. Calculated harmonic vibrational frequencies (in cm^{-1}) and band assignment for acetonitrile and some reduced species adsorbed on Pt(111).

A	B	C	D	E
CH_3-CN	CH_3-C=ND	CH_3-DC-N	CH_3-DC=ND	CH_3-DC-ND
3072, str CH_3	3055, str CH_3	3068, str CH_3	3065, str CH_3	3060, str CH_3
3061, str CH_3	3049, str CH_3	3024, str CH_3	3033, str CH_3	2992, str CH_3
2980, str CH_3	2965, str CH_3	2948, str CH_3	2980, str CH_3	2925, str CH_3
1644, str CN	2504, str ND	2235, str CD	2476, str ND	2465, str ND
1413, asym bend CH_3	1533, str CN	1419, asym bend CH_3	2254, str CD	2181, str CD
1405, asym bend CH_3	1409, asym bend CH_3	1404, asym bend CH_3	1621, str CN	1413, asym bend CH_3
1329, sym bend CH_3 + str CC	1395, asym bend CH_3	1341, sym bend CH_3	1428, asym bend CH_3	1409, asym bend CH_3
1012, bend CCH	1333, sym bend CH_3 + str CC	1326, sym bend CH_3 + str CC	1416, asym bend CH_3	1339, sym bend CH_3 + str CC
	1121, bend CCH	1067, str CN + bend CH_3	1352, sym bend CH_3 + str CC	1140, strCCN
		1014, bend CCH	1138, str CC + bend CCN + bend CCH	1053, str CC + bend CH_3
			1045,bend CCH + bend CCN	1023, bend CCN + bend CCH

Table 2. Calculated harmonic frequencies (in cm^{-1}) and band assignments for oxygenated species related to acetonitrile, adsorbed on Pt(111).

F	G	H
CH_3-C=NOD	CH_3-DC=NOD	CH_3-DC-NOD
3099, str CH_3	3088, str CH_3	3064, str CH_3
3031, str CH_3	3035, str CH_3	3012, str CH_3
2963, str CH_3	2962, str CH_3	2939, str CH_3
2628, str OD	2289, str OD	2355, str OD
1558, str CN	2270, str CD	2188, str CD
1417, asym bend CH_3	1618, str CN	1412, asym bend CH_3
1403, asym bend CH_3	1426, asym bend CH_3	1410, asym bend CH_3
1331, sym bend CH_3	1421, asym bend CH_3	1337, sym bend CH_3 + str CC
1099, bend CH_3 + str CC	1350, sym bend CH_3 + str CC	1149, str CN + bend NOD
1049, bend CCH	1114, str CC + bend NCH	1064, bend CCH + bend NOD
	1086, bend NOD + bend CCH	1039, str CC + bend NOD
	1019, bend NOD + bend CCH	1018, bend CCH

4.2. Study of the effect of the presence of acetonitrile on the ORR

The ORR was investigated in the same conditions shown in the previous sections by means of cyclic voltammetry and using the HMRDE configuration. The comparison between the different acetonitrile concentrations in acidic and alkaline media for both Pt(111) and Pt(100) is shown in Fig. 9. The limiting current density decrease observed at potentials below 0.2 V vs. RHE was traditionally ascribed to hydrogen adsorption, which would occupy the O_2 adsorption sites preventing the scission of the O-O bond [42]. However, recent investigations for the hydrogen peroxide reduction reaction (HPRR) on Pt(111) at different pH values pointed out that this inhibition could be determined by the electrode surface charge and interfacial water structure [43]. As can be seen, in 0.1 M $HClO_4$, the onset potential is shifted to less positive values for both orientations as acetonitrile concentration is increased.

Additionally, when acetonitrile is present in the solution, the current density values near the onset potentials are much lower in the negative-going scan. The displacement of the onset potential is due to the presence of acetonitrile adsorbed species, which produces a steric inhibition by the occupation of Pt sites, as proposed in refs. [18-20]. The higher inhibition in the negative-going scan (solid line in Fig. 9) is in agreement with that observed for the cyclic voltammetry experiments in the absence of oxygen: some desorption of acetonitrile adsorbed species takes place at the most negative potentials, and hence there are less of those species in the positive-going scan. At high potentials, they are restored again being the steric effect higher in the negative-going scan.

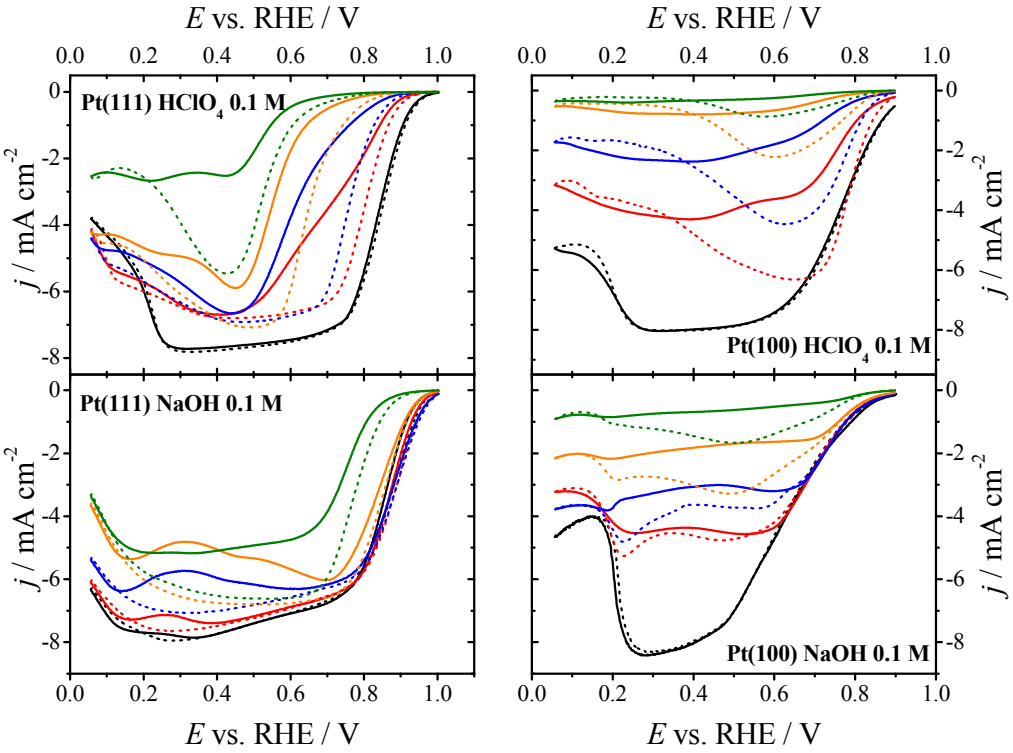

Figure 9. Voltammetric profiles for the ORR on Pt(111) and Pt(100) in 0.1 M $HClO_4$ + 0.1 M NaOH in the absence of acetonitrile and with different concentrations from 10^{-3} M to 1 M CH_3CN in O_2-saturated solutions. Black line: Without acetonitrile; red line: 10^{-3} M CH_3CN; blue line: 10^{-2} M CH_3CN; purple line: 0.1 M CH_3CN; green line: 1 M CH_3CN. Solid line: negative-going scan; dotted line: positive-going scan. Scan rate: 50 mV s^{-1}; rotation rate: 2500 rpm.

A decrease in the limiting current densities as acetonitrile concentration is increased can also be observed for both orientations, but interestingly this inhibition is

more important in the case of Pt(100). This is because the coverage of adsorbed species is higher for Pt(100) than for Pt(111), as inferred from the higher blockage of hydrogen adsorption/desorption region in the voltammetric profiles in the absence of O_2.

In alkaline media, some important differences can be observed. Firstly, the differences between the negative and the positive-going scans are less important, especially for the lower concentrations of acetonitrile. Furthermore, the onset potential is shifted to slightly more positive values for 10^{-3} M and 10^{-2} M CH_3CN on Pt(111) in comparison to the case in absence of acetonitrile. These results indicate that the coverage of adsorbed acetonitrile species is lower in alkaline media and therefore the blocking effect is much less evident. The small improvement on the onset potential could be due to the formation in lesser extent of the Pt oxides, together with its shift to more positive potentials in the presence of acetonitrile, as can be seen in Fig. S3. An analogous behavior was observed for polycrystalline Pt in acidic media for low concentrations of acetonitrile.[18] A stronger inhibition, with lower limiting current densities, is also observed for Pt(100) in alkaline media.

The determination of kinetic parameters for the ORR from Tafel slope analyses was carried out for the lowest concentration of acetonitrile in order to study a possible catalytic effect. Kinetic current densities (j_k) at a given potential were calculated by using the Koutecky-Levich equation (3) from the intercept at the y-axis of the j^{-1} *vs* $\omega^{-1/2}$ plot:

$$(3)\ \frac{1}{j} = \frac{1}{j_k} + \frac{1}{0.62nFD^{2/3}\nu^{-1/6}C^b\omega^{1/2}}$$

where F is the Faraday constant, D is the diffusion coefficient of O_2, ν is the kinematic viscosity of the solution, C^b is the bulk concentration of O_2 and ω is the rotation rate. Fig. S4 shows an example of a HMRDE experiment for different rotation rates: the data

between 0.85 and 0.90 V were used in order to calculate the correspondent Tafel slopes and the results are shown in Fig. 10 and Table 3.

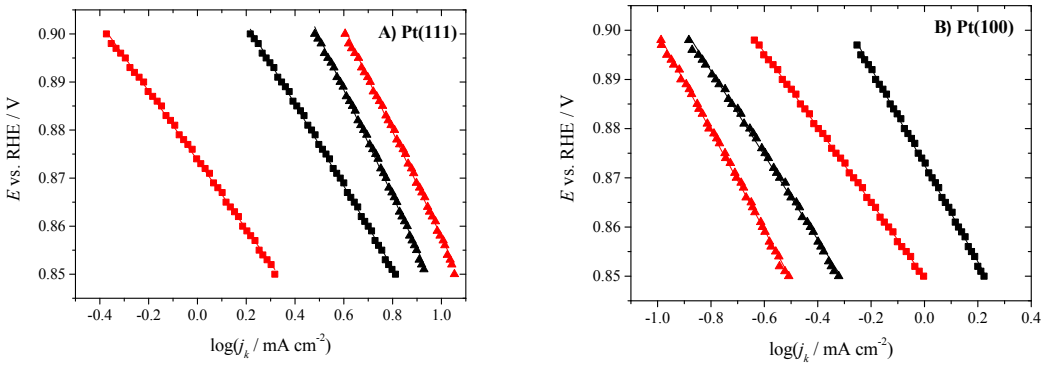

Figure 10. Tafel plots for the ORR on (A) Pt (111) and (B) Pt(100) in 0.1 M $HClO_4$ and 0.1 M NaOH O_2-saturated solutions in the absence and with 10^{-3} M CH_3CN. Black squares: 0.1 M $HClO_4$: 0.1 M $HClO_4$: red squares: 0.1 M $HClO_4$ + 10^{-3} M CH_3CN; black triangles: 0.1 M NaOH; red triangles: 0.1 M NaOH + 10^{-3} M CH_3CN.

Table 3. Tafel slope values for the ORR on Pt (111) and Pt(100) in 0.1 M $HClO_4$ and 0.1 M NaOH in the absence and with 10^{-3} M CH_3CN.

Pt(111)	**Tafel slope / mV**	
	0.1 M $HClO_4$	**0.1 M NaOH**
Without CH_3CN	85	111
[CH_3CN] = 10^{-3} M	72	110
Pt(100)	**Tafel slope / mV**	
	0.1 $HClO_4$	**0.1 NaOH**
Without CH_3CN	98	86
[CH_3CN] = 10^{-3} M	76	100

Lower Tafel slope values were obtained when 10^{-3} M CH_3CN is present in the case of 0.1 M $HClO_4$. This indicates a possible catalytic effect of the adsorbed acetonitrile on the mechanism for the ORR in acidic electrolyte media. The differences in the Tafel slopes values with the previous literature[21] are due to in this work the working electrodes are well-oriented surfaces with a different behaviour respect to a polyoriented material.

The fraction of formed H_2O_2 as side reaction product is interesting in order to prepare catalysts more selective in presence of contaminants. In this case, the fraction of H_2O_2 is estimated from the involved number of electrons calculated from the Levich equation (denominator in the last term of equation 3) using the limiting current densities. Results are presented in Table 4.

Table 4. Fraction of produced H_2O_2 for potentials corresponding to j_{lim} on Pt (111) and Pt(100) in 0.1 M $HClO_4$ and 0.1 M NaOH in the absence and with different concentrations of CH_3CN.

Pt(111)	**% H_2O_2**	
[CH_3CN] / M	**0.1 M $HClO_4$**	**0.1 M NaOH**
10^{-3}	17	6
10^{-2}	18	20
0.1	32	24
1	71	34

Pt(100)	**% H_2O_2**	
[CH_3CN] / M	**0.1 M $HClO_4$**	**0.1 M NaOH**
10^{-3}	47	45
10^{-2}	70	55
0.1	90	74
1	95	90

Results point out that more H_2O_2 is produced for Pt(100) than for Pt(111), and its formation is higher in acidic than in alkaline media. In conclusion, the formation of H_2O_2 in the presence of contaminants will be more favoured on Pt(100) in acidic media.

5. Conclusions

Adsorption and surface processes of acetonitrile on Pt(111) and Pt(100) have been thoroughly studied in aqueous acid and alkaline solutions in the presence of acetonitrile by means of cyclic voltammetry, in-situ infrared spectroscopy and, in the case of Pt(111), DFT calculations. These calculations have been carried out for acetonitrile-derived adspecies formed by hydroxylation of the nitrogen atom and by reduction of the CN bond to yield new CH and NH bonds. Most of the species studied, including acetonitrile itself, were bonded to the surface through both the C and N atoms

of the original nitrile moiety, while keeping the CN bond essentially parallel to the metal surface. All the adsorption geometries found with the nitrogen atom bonded to more than a surface Pt atom are significantly less stable than their respective chemical isomers where the N atom is linked to one surface Pt. Only two of the species studied have a unidentate configuration, with the N atom on top of a surface metal atom. These two species, that result from the addition of a hydrogen (or deuterium) atom to the central C atom, are the only ones that can explain the experimental observation of bands in the range 1500-1650 cm^{-1}, as their CN bonds (and transition dipole) have a significant component in the direction perpendicular to the surface (surface selection rule). The calculated frequencies for the undeuterated methyl groups are very similar for all the adspecies considered, in the range 1403-1428 cm^{-1} for the asymmetric CH_3 bendings, and 1326-1352 cm^{-1} for the symmetric CH_3 bending. These small differences do not allow a univocal assignment of the experimental bands observed in the range 1300-1500 cm^{-1} to one of the considered species.

In general, results reported in this work indicate that acetonitrile-related species can adsorb in the whole studied range from 0.06 to 0.90 V, and at potentials above 0.60 V rehybridized acetonitrile is transformed into a hydroxylated intermediate bonded to Pt through an electron donating bond. These species are reduced at intermediate potentials to form a reduced intermediate. The latter species can be further reduced and desorbed to the solution. Voltammetric results show that the degree of surface blockage by species coming from acetonitrile is higher on Pt(111) than on Pt(100) and it is much lower in alkaline media than in acidic solution.

The presence of surface species as deduced from the characterization studies significantly influences the ORR in these conditions. In acidic media the onset potential is shifted to less positive potentials for both orientations as the concentration of

acetonitrile is increased. The limiting current density also diminishes progressively but the inhibition is stronger in the case of Pt(100) because of the higher coverage of acetonitrile in this case. Regarding the results in alkaline media, the onset potential is slightly more positive for low concentrations of acetonitrile probably due to an inhibition of Pt oxides formation. A behavior similar to that found in acidic media is observed for the limiting current density. Tafel slope analyses show that values are lower for 10^{-3} M CH_3CN in acidic media because of a catalytic effect of adsorbed acetonitrile intermediate.

The present work contributes to clarify the surface electrochemical processes that take place during acetonitrile adsorption on Pt and it has analyzed the effects of acetonitrile on the ORR, which will be helpful to the preparation of new electrocatalysts in order to alleviate practical problems in real fuel cells.

Supporting Information

The Supporting Information shows additional cyclic voltammetry results in the absence of oxygen for Pt(111) in 0.1 M $HClO_4$ and 10^{-3} M CH_3CN in order to obtain more information about the acetonitrile adsorption processes (Figures S1 and S2). More concretely, it shows different consecutive cycles and results with a different initial potential. Figure S3 for Pt(111) in 0.1 M NaOH is also presented in order to show how the oxide formation region changes with the addition of acetonitrile. Figure S4 gathers measurements at different rotation speeds for the ORR on Pt(111) in 0.1 M $HClO_4$ and 10^{-3} M CH_3CN.

Acknowledgments

This work has been financially supported by the MCINN-FEDER (Spain) through project CTQ2016-76221-P. VBM thankfully acknowledges to MINECO the award of a predoctoral grant (BES-2014-068176, project CTQ2013-44803-P) and a student stay grant (EEBB-I-16-11656).

References

(1) Wroblowa, H. S.; Pan, Y.-C.; Razumney, G. Electroreduction of oxygen. *J. Electroanal. Chem.* **1976**, *69*, 195-201.

(2) Gómez-Marín, A. M.; Rizo, R.; Feliu, J. M. Oxygen reduction reaction at Pt single crystals: a critical overview. *Catal. Sci. Technol.* **2014**, *4*, 1685-1698.

(3) Gómez-Marín, A. M.; Rizo, R.; Feliu, J. M. Some reflections on the understanding of the oxygen reduction reaction at Pt(111). *Beilstein J Nanotech* **2013**, *4*, 956-967.

(4) Gómez-Marín, A. M.; Feliu, J. M. New Insights into the Oxygen Reduction Reaction Mechanism on Pt(111): A Detailed Electrochemical Study. *ChemSusChem* **2013**, *6*, 1091-1100.

(5) Briega-Martos, V.; Herrero, E.; Feliu, J. M. Effect of pH and water structure on the oxygen reduction reaction on platinum electrodes. *Electrochim. Acta* **2017**, *241*, 497-509.

(6) St-Pierre, J.; Zhai, Y.; Angelo, M. S. Effect of selected Airborne Contaminants on PEMFC Performance. *J. Electrochem. Soc.* **2014**, *161*, F280-F290.

(7) Angerstein-Kozlowska, H.; Macdougall, B.; Conway, B. E. Electrochemisorption and Reactivity of Nitriles at Platinum Electrodes and the Anodic H Desorption Effect. *J. Electroanal. Chem.* **1972**, *39*, 287-313.

(8) Morin, S.; Conway, B. E. Surface structure dependence of reactive chemisorption of acetonitrile on single-crystal Pt surfaces. *J. Electroanal. Chem.* **1994**, *376*, 135-150.

(9) Morin, S.; Conway, B. E.; Edens, G. J.; Weaver, M. J. The reactive chemisorption of acetonitrile on Pt(111) and Pt(100) electrodes as examined by in situ infrared spectroscopy. *J. Electroanal. Chem.* **1997**, *421*, 213-220.

(10) Marinkovic, N. S.; Hetch, M.; Loring, J. S.; Fawcett, W. R. A SNIFTIRS study of the diffuse double layer at single crystal platinum electrodes in acetonitrile. *Electrochim. Acta* **1996**, *41*, 641-651.

(11) Andrews, M. A.; Kaesz, H. D. Reversible hydrogenation and dehydrogenation of cluster bound acimidoyl and alkylidenimido groups. Synthesis of complexes containing triply bridging nitrene and nitrile ligands. *J. Am. Chem. Soc.* **1979**, *101*, 7255-7259.

(12) Sexton, B. A.; Avery, N. R. Coordination of acetonitrile (CH_3CN) to platinum (111): Evidence for an η^2(C, N) species. *Surf. Sci.* **1983**, *129*, 21-36.

(13) Rudnev, A. V.; Molodkina, E. B.; Danilov, A. I.; Polukarov, Y. M.; Berná, A.; Feliu, J. M. Adsorption behavior of acetonitrile on platinum and gold electrodes of various structures in solution of 0.5 M H_2SO_4. *Electrochim. Acta* **2009**, *54*, 3692-3699.

(14) Suarez-Herrera, M. F.; Costa-Figueiredo, M.; Feliu, J. M. Voltammetry of Basal Plane Platinum Electrodes in Acetonitrile Electrolytes: Effect of the Presence of Water. *Langmuir* **2012**, *28*, 5286-5294.

(15) Ledezma-Yanez, I.; Díaz-Morales, O.; Figueiredo, M. C.; Koper, M. T. M. Hydrogen Oxidation and Hydrogen Evolution on a Platinum Electrode in Acetonitrile. *ChemElectroChem* **2015**, *2*, 1612-1622.

(16) Ledezma-Yanez, I.; Wallace, W. D. Z.; Sebastián-Pascual, P.; Climent, V.; Feliu, J. M.; Koper, M. T. M. Interfacial water reorganization as a pH-dependent descriptor of the hydrogen evolution rate on platinum electrodes. *Nature Energy* **2017**, *2*, 17031-17037.

(17) Markovits, A.; Minot, C. Theoretical study of the acetonitrile flip-flop with the electric field orientation: adsorption on a Pt(111) electrode surface. *Catalysis Letters* **2003**, *91*, 225-234.

(18) Pašti, I. A.; Marković, A.; Gavrilov, N.; Mentus, S. V. Adsorption of Acetonitrile on Platinum and its Effects on Oxygen Reduction Reaction in Acidic Acidic Aqueous Solutions—Combined Theoretical and Experimental Study. *Electrocatalysis* **2016**, *7*, 235-248.

(19) Srejić, I.; Smiljanić, M.; Rakočević, Z.; Štrbac, S. Oxygen Reduction on Polycrystalline Pt and Au Electrodes in Perchloric Acid Solution in Presence of Acetonitrile. *Int. J. Electrochem. Sci.* **2011**, *6*, 3344-3354.

(20) Smiljanić, M. L.; Srejić, I. L.; Marinović, V. M.; Rakočević, Z. L.; Štrbac, S. B. Inhibiting effect of acetonitrile on oxygen reduction on polycrystalline Pt electrode in sodium chloride solution. *Hemijska Industrija* **2012**, *66*, 327-333.

(21) Ge, J.; St-Pierre, J.; Zhai, Y. PEMFC cathode catalyst contamination evaluation with a RRDE-Acetonitrile. *Electrochim. Acta* **2014**, *134*, 272-280.

(22) Reshetenko, T. V.; St-Pierre, J. Study of the acetonitrile poisoning of platinum cathodes on proton exchange membrane fuel cell spatial performance using a segmented cell system. *J. Power Sources* **2015**, *293*, 929-940.

(23) Korzeniewski, C.; Climent, V.; Feliu, J. M. Electrochemistry at Platinum Single Crystal Electrodes. In *Electroanalytical Chemistry: A Series of Advances*; Bard, A. J., Zoski, C., Eds.; CRC Press: Boca Raton, 2012; Vol. 24; pp 75-169.

(24) Clavilier, J.; Armand, D.; Sun, S. G.; Petit, M. Electrochemical adsorption behaviour of platinum stepped surfaces in sulphuric acid solutions *J. Electroanal. Chem.* **1986**, *205*, 267-277.

(25) Feliu, J. M.; Rodes, A.; Orts, J. M.; Clavilier, J. The problem of surface order of Pt single-crystals in electrochemistry. *Polish Journal of Chemistry* **1994**, *68*, 1575-1595.

(26) Perdew, J. P.; Burke, K.; Ernzerhof, M. Generalized Gradient Approximation Made Simple. *Phys. Rev. Lett.* **1996**, *77*, 3865-3868.

(27) Perdew, J. P.; Burke, K.; Ernzerhof, M. Generalized Gradient Approximation Made Simple [Phys. Rev. Lett. 77, 3865 (1996)]. *Phys. Rev. Lett.* **1997**, *78*, 1396-1396.

(28) Kresse, G.; Hafner, J. *Ab initio* molecular dynamics for liquid metals. *Phys. Rev. B* **1993**, *47*, 558-561.

(29) Kresse, G.; Hafner, J. *Ab initio* molecular-dynamics simulation of the liquid-metal–amorphous-semiconductor transition in germanium. *Phys. Rev. B* **1994**, *49*.

(30) Eichler, A.; Hafner, J.; Kresse, G.; Furthmuller, J. Relaxation and electronic surface states of rhodium surfaces. *Surf. Sci.* **1996**, *352*, 689-692.

(31) Kresse, G.; Furthmüller, J. Efficiency of ab-initio total energy calculations for metals and semiconductors using plane-wave basis set. *Comp. Mater. Sci.* **1996**, *6*, 15-50.

(32) Blöchl, P. E. Projector augmented-wave method. *Phys. Rev. B* **1994**, *50*, 17953-17979.

(33) Kresse, G.; Joubert, D. From ultrasoft pseudopotentials to the projector augmented-wave method. *Phys. Rev. B* **1999**, *59*, 1758-1775.

(34) Monkhorst, H. J.; Pack, J. D. Special points for Brillouin-zone integrations. *Phys. Rev. B* **1976**, *13*, 5188-5192.

(35) Methfessel, M.; Paxton, A. T. High-precision sampling for Brillouin-zone integration in metals. *Phys. Rev. B* **1989**, *40*, 3616-3621.

(36) Cheuquepán, W.; Rodes, A.; Orts, J. M.; Feliu, J. M. Spectroelectrochemical detection of specifically adsorbed cyanurate anions at gold electrodes with (111) orientation in contact with cyanate and cyanuric acid neutral solutions. *J. Electroanal. Chem.* **2017**, *800*, 167-175.

(37) Cheuquepán, W.; Orts, J. M.; Rodes, A. Hydroxyurea electrooxidation at gold electrodes. In situ infrared spectroelectrochemical and DFT characterization of adsorbed intermediates. *Electrochim. Acta* **2017**, *246*, 951-962.

(38) Schaftenaar, G.; Noordik, J. H. Molden: A pre- and post-processing program for molecular and electronic structures. *J. Comput. Aided Mol. Des.* **2000**, *14*, 123-134.

(39) Jmol: an open-source Java viewer for chemical structures in 3D, in http:\\www.jmol.org, 2015.

(40) Strmcnik, D.; Escudero-Escribano, M.; Kodama, K.; Stamenkovic, V. R.; Cuesta, A.; Marković, N. M. Enhanced electrocatalysis of the oxygen reduction reaction based on patterning of platinum surfaces with cyanide. *Nat. Chem.* **2010**, *2*, 880-885.

(41) Greenler, R. G. Infrared Study of Adsorbed Molecules on Metal Surfaces by Reflection Techniques. *J. Chem. Phys.* **1966**, *44*, 310-315.

(42) Markovic, N. M.; Gasteiger, H. A.; Ross, P. N. Oxygen Reduction on Platinum Low-Index Single-Crystal Surfaces in Sulfuric-Acid-Solution - Rotating Ring-Pt(hkl) Disk Studies. *J. Phys. Chem.* **1995**, *99*, 3411-3415.

(43) Briega-Martos, V.; Herrero, E.; Feliu, J. M. The inhibition of hydrogen peroxide reduction at low potentials on Pt(111): Hydrogen adsorption or interfacial charge? *Electrochem. Commun.* **2017**, *85*, 32-35.

TOC graphic

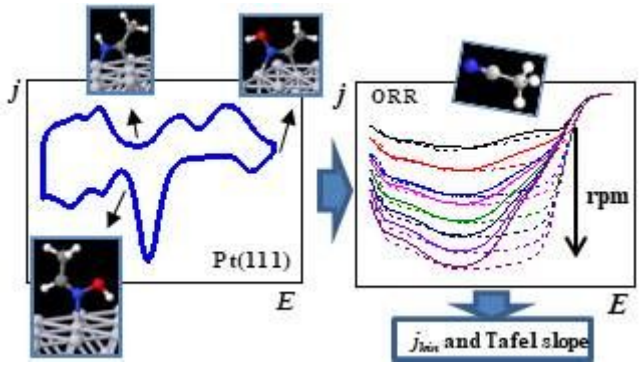

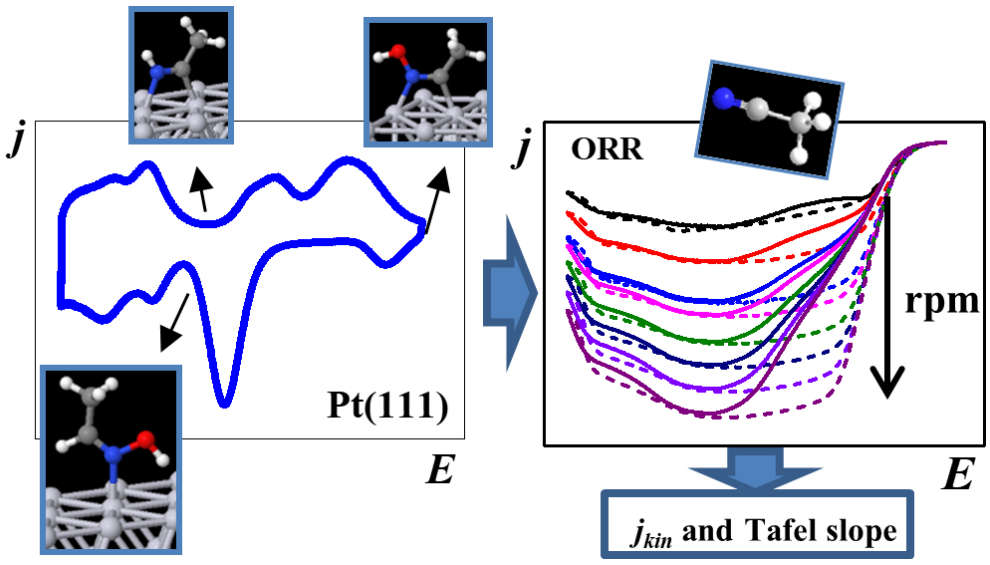

85x47mm (300 x 300 DPI)